

Combined Conduction and Correlated-Radiation Heat Transfer in Packed Beds

K. Kamiuto,* M. Iwamoto,† and Y. Nagumo†
Oita University, Oita 870-11, Japan

A quasihomogeneous model for heat transfer in a plane-parallel packed bed of opaque spheres is presented. The proposed model takes into account the variable porosity distribution within a packed bed and the correlated radiative properties of packed spheres having gray diffuse surfaces. On the basis of the proposed model, combined conductive and radiative heat transfer through comparatively thin packed layers of cordierite spheres or oxidized steel spheres are analyzed numerically and the obtained results are compared with the experimental ones. Additionally, the adequacy of a simplified analytical formula for the total effective thermal conductivities of a packed bed is discussed. It is found that the detailed theoretical model accurately predicts the heat transfer characteristics and the temperature profiles of the plane-parallel packed beds, and the predictions derived from the approximate formula well-correlate with the present experimental data for the total effective thermal conductivities.

Nomenclature

d_p	= mean diameter of packed spheres, m
f_v	= volume fraction of a packed bed
G	= incident radiation, W/m ²
\bar{g}	= asymmetry factor of the phase function of a packed bed
\bar{g}_s	= asymmetry factor of the surface-scattering phase function of diffuse spheres, $-\frac{4}{3}$
I	= intensity of radiation, W/m ² -sr
I_b	= intensity of blackbody radiation, W/m ² -sr
k_a	= thermal conductivity of a continuous phase, W/mk
k_{app}	= approximate total effective thermal conductivity defined by Eq. (28), W/mk
k_{eff}	= total effective thermal conductivity of a packed bed, W/mk
k_m	= effective thermal conductivity by conduction alone, W/mk
k_s	= thermal conductivity of a dispersed phase, W/mk
N_R	= conduction-radiation parameter
\tilde{N}_R	= modified conduction-radiation parameter
n_p	= number density of packed spheres, beads/m ³
$P_s(\Theta)$	= surface-scattering phase function
$P_s(\mu, \mu')$	= azimuthally averaged surface-scattering phase function
q_i	= total heat flux, W/m ²
T	= temperature, K
\hat{T}	= temperature defined by $T/1000$, K
T_m	= mean bed temperature defined by $(T_1 + T_2)/2$, K
y	= distance from the hot boundary, m
y_0	= thickness of a packed bed, m
z	= distance from a boundary surface, m
β	= extinction coefficient of a packed bed, m ⁻¹
$\tilde{\beta}$	= transformed extinction coefficient, m ⁻¹
γ_2	= extinction coefficient ratio

ϵ	= total hemispherical emissivity
η	= dimensionless distance from the hot boundary, y/y_0
Θ	= scattering angle
θ	= dimensionless temperature, T/T_1
θ_2	= dimensionless temperature of the cold boundary, T_2/T_1
κ	= quantity defined by k_s/k_a
λ_m	= dimensionless effective thermal conductivity, $k_m/k_s(T_1)$
λ_w	= representative wavelength of radiation within a bed, μm
ξ	= dimensionless distance from a boundary surface, z/d_p
ξ_0	= dimensionless packed bed thickness, y_0/d_p
ξ_1	= quantity defined by $\xi - 0.6$
ρ	= total hemispherical reflectivity
σ	= Stefan-Boltzmann's constant, W/m ² K ⁴
σ_a	= absorption coefficient of a packed bed, m ⁻¹
τ_0	= transformed optical thickness
ϕ	= porosity
χ	= dimensionless incident radiation, $G/\sigma T_1^4$
ω	= albedo
$\tilde{\omega}$	= transformed albedo

Subscripts

1	= hot boundary
2	= cold boundary

Superscripts

*	= dimensionless quantity
-	= mean quantity

Introduction

STUDY of simultaneous conduction and radiation heat transfer through a packed layer of solid spheres is of practical importance in connection with thermal designs of pebble-bed-type gas-cooled reactors, catalytic converters, etc., and there exists much literature on this subject.¹⁻⁵ Generally, theoretical models adopted in these previous studies may be classified into two categories: 1) cell model,^{1,2} and 2) quasihomogeneous model.³⁻⁵ Of these, the former model could not take into account the long-range effects of radiative transfer through the voids of a packed bed, and therefore, leads to serious errors in evaluating the heat transfer characteristics of a comparatively thin packed bed. Moreover, this model

Received Dec. 5, 1991; revision received Aug. 10, 1992; accepted for publication Aug. 10, 1992. Copyright © 1992 by the American Institute of Aeronautics and Astronautics, Inc. All rights reserved.

*Professor, Department of Production Systems Engineering, Dan-noharu 700.

†Graduate Student, Department of Production Systems Engineering.

involves a lot of adjustable parameters that must be determined experimentally. On the other hand, the quasihomogeneous model readily enables us to take into account the long-range effect of radiative transfer because, within the framework of this model, radiative transfer through a packed bed is governed by the equation of transfer, and thus, radiative transports such as radiative heat flux may be accurately evaluated even for a comparatively thin packed bed by solving numerically the equation of transfer. However, at that time, the radiative properties appearing in the equation of transfer are required to be known, and it is essential for the quasihomogeneous model to describe these quantities in terms of void fraction, particle size, and surface reflectivity of the particles. Unfortunately, uncorrelated-scattering theory such as Mie's theory⁶ is not appropriate for this purpose because this theory fails to elucidate experimental results for the radiative properties of packed beds,⁷ and the correlated-scattering theory⁸ should be utilized.

In the present study, first, a quasihomogeneous model for packed-bed heat transfer at high temperatures is described. Then, to discuss the validity of the theoretical analyses based on this model, simultaneous conduction and radiation heat transfer within comparatively thin packed layers of cordierite beads or oxidized steel beads are studied both experimentally and theoretically. In the experiments, utilizing a guarded hot-plate-type apparatus, the temperature profiles and the heat transfer characteristics of two kinds of packed beds were measured by varying the hot boundary temperatures from 320 to 870 K or 1070 K. In the theoretical analyses, both the energy equation and the equation of transfer were derived from the proposed model and were solved numerically using finite differences under conditions corresponding to the experiments.

Finally, predictions based on a simplified analytical formula⁹ for the total effective thermal conductivities of a packed bed are compared with the present experimental data.

Theoretical Model

Basic Assumptions

The present model is based on the following assumptions:

- 1) The packed bed consists of large solid spheres and a gas and is bounded by two separate infinite plane-parallel plates.
- 2) The packed bed is continuous for heat transfer and is at steady state.
- 3) Heat transfer through the packed bed is due to conduction and radiation.
- 4) Local porosity within the packed bed varies with distance from both boundaries alone, and the porosity distribution is symmetric with respect to the midplane of the packed bed.
- 5) The two boundaries of the packed bed are maintained at constant but different temperatures and are considered to be gray diffuse emitters and reflectors.
- 6) The total hemispherical emissivity of the hot boundary depends on temperature, while that of the cold boundary is independent of temperature and is assumed to be unity.
- 7) Packing spheres are opaque and have gray diffuse surfaces, and the radiative properties of a packed bed can be predicted on the basis of the correlated-scattering theory.⁸
- 8) The thermal conductivities of a gas and solid spheres depend on temperature.
- 9) A local thermodynamic equilibrium exists within the packed bed.

Governing Equations

Under the foregoing assumptions, the energy equation can be written as follows:

$$\frac{d}{dy} \left[k_m(y) \frac{dT}{dy} \right] = \sigma_a [4\sigma T^4(y) - G(y)] \quad (1)$$

where $k_m(y)$ represents the effective thermal conductivity of a packed bed at distance y from the hot boundary, and $G(y)$ the incident radiation defined by

$$2\pi \int_{-1}^1 I(y, \mu) d\mu$$

Here, $I(y, \mu)$ denotes the intensity of radiation.

The boundary conditions for Eq. (1) are

$$y = 0: T = T_1, y = y_0: T = T_2 (< T_1) \quad (2)$$

The transformed equation of transfer pertinent to the present system^{8,10} can be given as

$$\mu \frac{\partial I(y, \mu)}{\partial y} + \tilde{\beta}(y) I(y, \mu) = \left[\frac{\tilde{\omega}(y) \tilde{\beta}(y)}{2} \right] \int_{-1}^1 P_s(\mu, \mu') \cdot I(y, \mu') d\mu' + \tilde{\beta}(y) [1 - \tilde{\omega}(y)] I_b(y) \quad (3)$$

The boundary conditions for Eq. (1) are as follows:

$$\begin{aligned} I(0, \mu > 0) &= \varepsilon_1(T_1) \left(\frac{\sigma T_1^4}{\pi} \right) \\ &+ 2[1 - \varepsilon_1(T_1)] \int_0^1 I(0, -\mu') \mu' d\mu' \\ I(y_0, \mu < 0) &= (\sigma T_2^4 / \pi) \end{aligned} \quad (4)$$

Multiplying both sides of Eq. (1) by $y_0^3/k_s(T_1)T_1$, we can obtain the following dimensionless equation of conservation of energy:

$$\begin{aligned} \left(\frac{d\lambda_m}{d\eta} \right) \left(\frac{d\theta}{d\eta} \right) + \lambda_m(\eta) \frac{d^2\theta}{d\eta^2} \\ = \left[\frac{\tilde{\tau}_0(\eta)}{N_R} \right] [1 - \tilde{\omega}(\eta)] \left[\theta^4(\eta) - \frac{\chi(\eta)}{4} \right] \end{aligned} \quad (5)$$

The corresponding boundary conditions may also be rewritten as

$$\eta = 0: \theta = 1, \eta = 1: \theta = \theta_2 \quad (6)$$

Furthermore, dividing both sides of Eq. (3) by $\sigma T_1^4/\pi$ results in

$$\begin{aligned} \mu \frac{\partial I^*(\eta, \mu)}{\partial \eta} + \tilde{\tau}_0(\eta) I^*(\eta, \mu) &= \tilde{\tau}_0(\eta) [1 - \tilde{\omega}(\eta)] \theta^4(\eta) \\ &+ \left[\frac{\tilde{\tau}_0(\eta) \tilde{\omega}(\eta)}{2} \right] \int_{-1}^1 P_s(\mu, \mu') I^*(\eta, \mu') d\mu' \end{aligned} \quad (7)$$

The boundary conditions for Eq. (7) can also be rewritten in the dimensionless form

$$\begin{aligned} I^*(0, \mu) &= \varepsilon_1(\theta_1) + 2[1 - \varepsilon_1(\theta_1)] \int_0^1 I^*(0, -\mu') \mu' d\mu' \\ I^*(1, -\mu) &= \theta_2^4 \end{aligned} \quad (8)$$

where $\mu > 0$.

The dimensionless quantities appearing in the above equations are defined as follows:

$$\begin{aligned} I^*(\eta, \mu) &= I(y, \mu) / (\sigma T_1^4 / \pi), \quad N_R = k_s(T_1) / 4\sigma T_1^3 y_0, \quad \eta = y / y_0 \\ \theta &= T / T_1, \quad \theta_2 = T_2 / T_1, \quad \lambda_m(\eta) = k_m(y) / k_s(T_1) \\ \tilde{\tau}_0(\eta) &= \tilde{\beta}(y) y_0, \quad \chi(\eta) = \tilde{\omega}(y) / \sigma T_1^4 \end{aligned} \quad (9)$$

Effective Thermal Conductivity

To actually solve Eq. (5), λ_m needs to be known. For this purpose, we utilize Bruggeman's effective medium theory.^{11,12}

In accord with this theory, λ_m is given by Eq. (10) for a gas-solid packed bed

$$\lambda_m = [k_a/k_s(T_1)]\{(\kappa - 1)\kappa^{1/3}\phi[\sqrt[3]{(-1 + \sqrt{A})/2} - \sqrt[3]{(1 + \sqrt{A})/2}] + \kappa\} \quad (10)$$

where $A = 1 + (\frac{4}{27})\phi^3(\kappa - 1)^3/\kappa^2$, and $\kappa = k_s/k_a$.

Porosity Distribution Function

The porosity distribution within a packed bed must be described explicitly, since Eqs. (5), (7), and (10) involve the porosity as a parameter. We utilized the porosity distribution function mathematically represented by Eqs. (11) and (12), which were derived from the experimental data of Ridgeway and Turback.^{13,14}

For $0 \leq \xi \leq 0.6$

$$\phi(\xi) = 1 - 3.10036\xi + 3.70243\xi^2 - 1.24612\xi^3 \quad (11)$$

For $0.6 \leq \xi \leq 0.5\xi_0$

$$\phi(\xi) = -0.1865 \exp(-0.22\xi_1^{1.5})\cos(7.66\xi_1) + 0.39 \quad (12)$$

where $\xi_1 = \xi - 0.6$, $\xi = z/d_p$, and $\xi_0 = y_0/d_p$. Here, ξ_0 must be greater than about 10.

Radiative Properties

Solution of the equation of transfer requires the radiative properties such as $\bar{\tau}_0$, $\bar{\omega}$, and $P_s(\mu, \mu')$ to be known. For usual packed bed conditions, the radiative properties cannot be given by simply summing the radiative properties of individual spheres in the same way as Mie's theory,⁶ and correlation between scatterers must be taken into account. Recently, one of the authors proposed a semi-empirical correlated-scattering theory,⁸ and showed the following:

1) A ratio of the extinction efficiency factor of packed spheres to that predicted from Mie's theory, i.e., 2, increases with the volume fraction of packed spheres f_v .

2) The asymmetry factor of the phase function of opaque packed spheres becomes small with increasing f_v : the backward scattering due to spheres within a bed is augmented by the presence of intercorrelation between packed spheres.

3) The scattering albedo decreases slightly as f_v increases.

On the basis of this correlated-scattering theory, the scaled radiative properties for a packed bed are described in the form

$$\begin{aligned} \bar{\tau}_0 &= \bar{\beta}y_0 = \pi d_p^2 n_p(y)[2\gamma_2(y) - 1]y_0/4 \\ &= 1.5(y_0/d_p)[1 - \phi(\eta)][2\gamma_2(\eta) - 1] \end{aligned} \quad (13)$$

$$\bar{\omega} = \rho(\eta) \quad (14)$$

$$P_s(\mu, \mu') = \int_0^{2\pi} P_s(\Theta) \frac{d\phi}{2\pi} \quad (15)$$

$$P_s(\Theta) = (8/3\pi)(\sin \Theta - \Theta \cos \Theta) \quad (16)$$

$$\gamma_2 = 1 + 1.5[1 - \phi(\eta)] - (\frac{1}{3})[1 - \phi(\eta)]^2 \quad (17)$$

where $P_s(\Theta)$ represents the surface-scattering phase function of a diffuse sphere.¹⁵ It should be stressed that these expressions hold under the conditions that packed spheres are opaque and have gray diffuse surfaces, and the size parameter of the spheres defined by $\pi d_p/\lambda_w$ is greater than about 100. Here, λ_w is given by $2897.6/T_m \mu\text{m}$. Moreover, the present correlated-scattering theory includes an uncorrelated-scattering case which may be observed in tenuous media, and for such a case γ_2 becomes unity. The present uncorrelated-scattering cal-

culations are carried out by assuming $\gamma_2 = 1$ in Eq. (13), and utilizing Eqs. (14) and (15).

Heat Transfer Characteristics

The total heat flux across a packed bed is calculated from

$$q_t = -k_m(y) \frac{dT}{dy} + 2\pi \int_{-1}^1 I(y, \mu) \mu d\mu \quad (18)$$

Multiplying both sides of Eq. (18) by $y_0/k_s(T_1)T_1$ yields

$$q_t^* = -\lambda_m(\eta) \frac{d\theta}{d\eta} + \left(\frac{1}{2N_R}\right) \int_{-1}^1 I^*(\eta, \mu) \mu d\mu \quad (19)$$

The mean total effective thermal conductivities of a packed bed between T_2 and T_1 can be evaluated by

$$\bar{k}_{\text{eff}} = \int_{T_2}^{T_1} k_{\text{eff}}(T) \frac{dT}{(T_1 - T_2)} = \frac{q_t^* k_s(T_1)}{1 - \theta_2} \quad (20)$$

Similarly, \bar{k}_m is calculated from

$$\bar{k}_m = \int_{T_2}^{T_1} k_m(T) \frac{dT}{(T_1 - T_2)} \quad (21)$$

Numerical Methods

Obviously, it is not amenable to obtain analytical solutions to Eqs. (5) and (7), and thus we must resort to numerical means. The energy equation was solved by an implicit finite difference method utilizing central differences for all derivatives, while the radiation term and one of the conduction terms, $(d\lambda_m/d\eta)(d\theta/d\eta)$, were treated as iterative ones. For the finite difference calculations of the energy equation, the thickness of a packed bed was divided into 2000 equally spaced increments, and thus the temperatures within a bed were obtained on the 1999 conduction lattice points. Furthermore, in order to evaluate the dimensionless incident radiation in Eq. (5), the equation of transfer was solved by Barkstrom's method¹⁶: a 20th Gaussian quadrature formula was used to evaluate the angular integral, and the optical thickness of a packed bed was divided into 400 equally spaced increments for depth discretization. Since the dimensionless incident radiations were directly obtainable only on the 401 radiation lattice points, the dimensionless incident radiations on the 1999 conduction lattice points were evaluated utilizing a cubic spline interpolation from the known dimensionless incident radiations on the radiation lattice points.

Actual computations have been proceeded according to the following procedures: first, to obtain a first approximation to $\theta(\eta)$, the equation of transfer was solved by Barkstrom's method, regarding the temperature field as known. We assumed $\theta^{(0)} = -(1 - \theta_2)\eta + 1$ as a first approximation to $\theta(\eta)$. Once $\chi(\eta)$ was obtained, the energy Eq. (5) can be readily solved with respect to θ as a set of tridiagonal simultaneous linear equations. Thereafter, the derived solution on θ was substituted into Eq. (7) to get a new solution of the equation of transfer. Similar computations were performed until the following criterion was satisfied:

$$|(\theta^{(n)} - \theta^{(n-1)})/\theta^{(n)}| < 10^{-3} \quad (22)$$

where the superscript n denotes the n th order approximation.

Experiment

Experimental Apparatus

The experimental apparatus utilized in the present study has almost the same structure and the same dimension as those described in Ref. 17, and therefore, we only refer to a point of difference. Two kinds of the hot end units ($0.3 \times 0.3 \text{ m}^2$)

were used: one was made of 0.005-m thick SUS316 plates, and another was made of 0.005-m thick SUS310 plates. On the other hand, the cold end unit was made of SUS316 plates and was coated with black flat paint. The SUS310 and SUS316 plates utilized here were oxidized at 1000 K for 10 h. The total hemispherical emissivities of the SUS316 plates⁵ were given by

$$\varepsilon_1 = 0.34456 + 0.48851\bar{T} - 0.16799\bar{T}^2 \quad (23)$$

while those of the SUS310 plates were described by

$$\varepsilon_1 = 0.031538 + 0.38714\bar{T} \quad (24)$$

The SUS310 plates were used for the steel bed, while the SUS316 plates were utilized for the cordierite bed. The total hemispherical emissivity of the cold boundary surface was assumed to be unity.

Packing Materials

Two kinds of solid spheres were used as packing materials, i.e., steel and cordierite ($2\text{MgO} \cdot 3\text{Al}_2\text{O}_3 \cdot 5\text{SiO}_2$). The carbon content of steel beads was 0.5 wt%. The mean void fraction of cordierite was 0.164. The mean diameter of the steel beads was 0.011 m and that of the cordierite beads was 0.00694 m. These beads were almost spherical in shape and their surfaces were diffuse. The total hemispherical reflectivities of the steel beads¹⁸ were assumed to be 0.2, irrespective of the temperature, while those of the cordierite beads¹⁹ were given by

$$\rho = 0.2695 - 1.749\bar{T} + 4.5495\bar{T}^2 - 3.6186\bar{T}^3 + 0.9418\bar{T}^4 \quad (25)$$

The thermal conductivities of steel²⁰ were approximated by

$$k_s = 57.705 - 11\bar{T} \quad (26)$$

The thermal conductivities of cordierite²¹ were given by

$$k_s = 1.7505 - 0.12597\bar{T} - 0.01501\bar{T}^2 + 0.0039789\bar{T}^3 \quad (27)$$

Experimental Procedures

Fourteen or ten chromel-alumel sheathed thermocouples of 2.3×10^{-3} m diam were vertically installed in the central part of the test section. The thickness and the porosity of the packed layer are shown in Table 1. The hot end units were placed in position, and the insulation was packed around the units to prevent heat losses. In each run, it took about 8 h to reach steady state, which was maintained for at least 1 h before measurements were made. The temperature of the hot boundary was varied from 320 to 870 K, while the temperature of the cold boundary was maintained within the approximate range of 290–320 K. All the experiments were done in air at atmospheric pressure.

Table 1 Characteristic values of the cordierite bed and the oxidized steel bed

	Cordierite beads	Steel beads
Mean diameter		
d_p (m)	6.94×10^{-3}	1.1×10^{-2}
Bed thickness		
y_0 (m)	0.086	0.108
y_0/d_p	12.4	9.82
Mean porosity		
ϕ	0.438	0.42

Results and Discussion

Temperature Profiles

Typical temperature profiles of the steel packed bed and the cordierite packed bed are shown in Figs. 1 and 2 where the theoretical predictions are denoted by solid lines. As seen from these figures, the theoretical temperature profiles are characterized by steep gradients at the walls and undulations over the whole bed. These are attributable to the fact that the local effective thermal conductivities of a packed bed vary in accord with the local porosity distribution through Eq. (10). Although there exists little discrepancy between theory and experiment, the agreement between them is acceptable within the accuracy of the present measurements.

Heat Transfer Characteristics

Results for the mean total effective thermal conductivities are shown in Figs. 3 and 4, where the numerical results based on the uncorrelated-scattering theory mentioned earlier are denoted by dot-dashed lines, and the exact numerical results are represented by solid lines. The agreement between the exact numerical results based on the correlated-scattering theory and the experimental ones is excellent, and this confirms the validity of the present analyses based on the proposed model. Moreover, these figures show that the numerical analyses based on the uncorrelated-scattering theory always overestimate the total effective thermal conductivities of the beds in comparison with the exact analyses based on the correlated-scattering theory. This is caused by the fact that the uncorrelated-scattering theory underestimates the optical thickness of a packed bed and simultaneously overestimates the forward

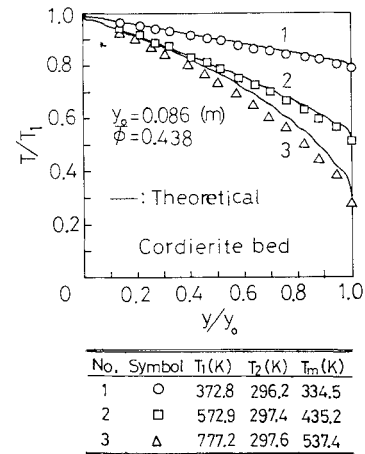


Fig. 1 Temperature profiles within a packed bed of cordierite spheres.

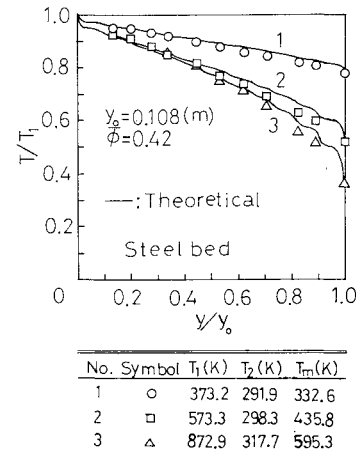


Fig. 2 Temperature profiles within a packed bed of oxidized steel spheres.

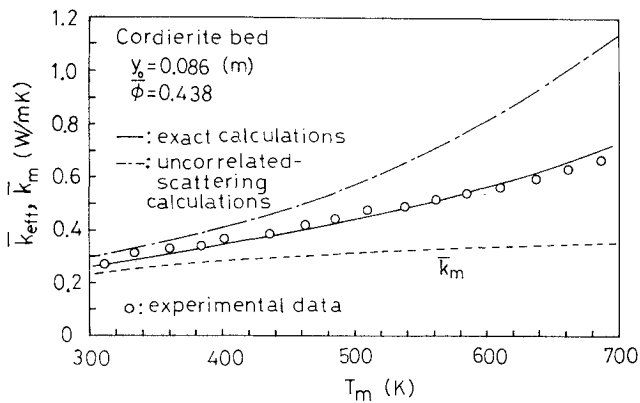


Fig. 3 Relation between mean total effective thermal conductivities and mean temperatures for a packed bed of cordierite spheres.

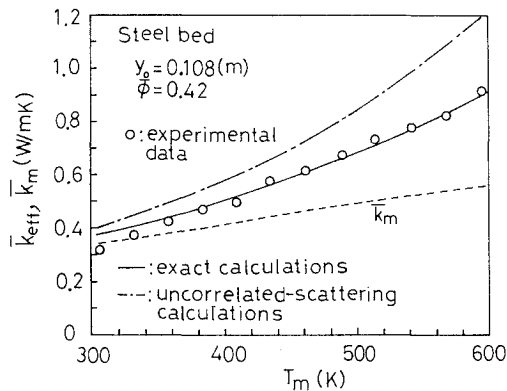


Fig. 4 Relation between mean total effective thermal conductivities and mean temperatures for a packed bed of oxidized steel spheres.

scattering due to packed spheres and, as a result, overestimates the contribution of radiation heat transfer in evaluating the total effective thermal conductivities.

However, it should be noted that in the case of thick non-absorbing media such as glass bead layers,²² the difference between the uncorrelated-scattering calculations and the correlated-scattering ones for the mean total effective thermal conductivities of the packed bed is negligible, because the interaction between conduction and radiation is intrinsically weak, and the effect of the increase in the extinction coefficient on radiation heat transfer is canceled by the enhancement of the forward scattering due to packed spheres.

Examination of an Analytical Formula for the Total Effective Thermal Conductivities of a Packed Bed

It is shown throughout the present study that the theoretical analyses based on the proposed model are accurate in predicting the heat transfer characteristics of a packed bed, but this never discounts the usefulness of an approximate analytical formula for the total effective thermal conductivity. Recently, we have derived an analytical formula, Eq. (28), utilizing the optically thick limit to the P_1 equations and the correlated-radiative properties of diffuse packing spheres, together with the constant porosity assumption

$$k_{app}(T_m)/k_a = k_m(T_m)/k_a + (\frac{1}{3})/[\tilde{N}_R(1 - \omega\bar{g})] \quad (28)$$

\tilde{N}_R is defined by

$$\tilde{N}_R = \beta k_a / 4\sigma T_m^3 \quad (29)$$

Unlike the aforementioned scaled radiative properties, the radiative properties appearing in Eq. (28) take into account the diffraction scattering due to individual spheres and are

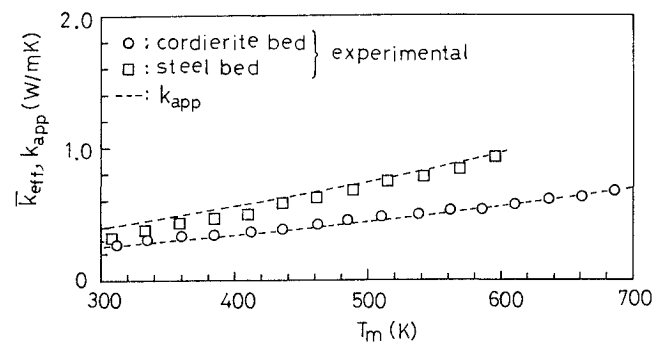


Fig. 5 Correlation between predictions derived from Eq. (28) and the present experimental results for the total effective thermal conductivities.

defined as

$$\beta = 3\gamma_2(1 - \phi)/d_p \quad (30)$$

$$\omega = [1 + (2\gamma_2 - 1)\rho]/2\gamma_2 \quad (31)$$

$$\bar{g} = [1 + (2\gamma_2 - 1)\rho\bar{g}_s]/[1 + (2\gamma_2 - 1)\rho] \quad (32)$$

Correlation between the present experimental data and the predictions derived from Eq. (28) is shown in Fig. 5. Strictly speaking, the mean total effective thermal conductivity \bar{k}_{app} defined by

$$\int_{T_2}^{T_1} k_{app}(T) \frac{dT}{(T_1 - T_2)}$$

should be used in Fig. 5, but $k_{app}(T_m)$ is shown instead of \bar{k}_{app} , because $k_{app}(T)$ can be well-approximated by a linear function of temperature as long as the present packed beds are concerned and, under this condition, \bar{k}_{app} is identical with $k_{app}(T_m)$. As seen from this figure, the agreement between prediction and experiment is satisfactory, and this justifies the use of Eq. (28), instead of the exact analyses, for predicting the total effective thermal conductivities of a plane-parallel packed bed with $y_0/d_p \geq 10$. The comparison between the predictions derived from Eq. (28) and other experimental data reported in the literature was made in Ref. 9.

Conclusions

The major conclusions that can be drawn from the present study are as follows:

- 1) The present packed-bed heat transfer model yields accurate results in predicting the mean total effective thermal conductivities and temperature profiles of a plane-parallel packed bed.
- 2) Simplified analytical formula for the total effective thermal conductivities of a packed bed, Eq. (28), well-correlates with the present experimental data.

References

- ¹Yagi, S., and Kunii, D., "Studies on Effective Thermal Conductivities in Packed Beds," *AIChE Journal*, Vol. 3, March 1957, pp. 373-381.
- ²Schotte, W., "Thermal Conductivities of Packed Beds," *AIChE Journal*, Vol. 6, Feb. 1960, pp. 63-67.
- ³Chen, J. C., and Churchill, S. W., "Radiant Heat Transfer in Packed Beds," *AIChE Journal*, Vol. 9, Jan. 1963, pp. 35-41.
- ⁴Chan, C. K., and Tien, C. L., "Radiative Transfer in Packed Spheres," *Journal of Heat Transfer*, Vol. 96, Feb. 1974, pp. 52-58.
- ⁵Kamiuto, K., and Iwamoto, M., "Analytical and Experimental Study of Combined Conductive and Radiative Heat Transfer Through a Layer of Glass Beads," *JSME International Journal, Series II*, Vol. 31, No. 3, 1988, pp. 537-544.
- ⁶Hottel, H. C., and Sarofim, A. F., "Radiative Transfer," Mc-

Graw-Hill, New York, 1967, p. 408.

⁷Kamiuto, K., "Study of the Scattering Regime Diagrams," *Journal of Thermophysics and Heat Transfer*, Vol. 4, No. 4, 1990, pp. 432-435.

⁸Kamiuto, K., "Radiative Properties of Packed-Sphere Systems Estimated by the Extended Emerging-Intensity Fitting Method," *Journal of Quantitative Spectroscopy and Radiative Transfer*, Vol. 47, No. 4, 1992, pp. 257-261.

⁹Kamiuto, K., "Analytical Formula for Total Effective Thermal Conductivities of Packed Beds," *Journal of Nuclear Science and Technology*, Vol. 28, No. 12, 1991, pp. 1153-1156.

¹⁰Kamiuto, K., "The Diffraction-Scattering Subtraction Method for Highly Anisotropic Scattering Problems," *Journal of Quantitative Spectroscopy and Radiative Transfer*, Vol. 40, No. 1, 1988, pp. 21-28.

¹¹Bruggeman, D. A., "Berechnung Verschiedenen Physikalischer Konstanten von Heterogenen Substanzen," *Annalen der Physik*, Vol. 24, May, pp. 636-679.

¹²Kamiuto, K., "Examination of Bruggeman's Theory for Effective Thermal Conductivities of Packed Beds," *Journal of Nuclear Science and Technology*, Vol. 27, No. 5, 1990, pp. 473-476.

¹³Ridgeway, K., and Turback, K. J., "Radial Voidage Variation in Randomly-Packed Beds of Spheres of Different Sizes," *Journal of Pharmacy and Pharmacology*, Vol. 18, Supplement, 1966, pp. 168S-

175S.

¹⁴Kamiuto, K., Nagumo, Y., and Iwamoto, M., "Mean Effective Thermal Conductivities of Packed-Sphere Systems," *Applied Energy*, Vol. 34, Feb. 1989, pp. 213-221.

¹⁵Siegel, R., and Howell, J. R., *Thermal Radiation Heat Transfer*, 2nd ed., Hemisphere, New York, 1981, pp. 581, 582.

¹⁶Barkstrom, B. R., "A Finite Difference Method for Solving Anisotropic Scattering Problems," *Journal of Quantitative Spectroscopy and Radiative Transfer*, Vol. 16, No. 6, 1976, pp. 725-739.

¹⁷Kamiuto, K., and Iwamoto, M., "Inversion Method for Determining Effective Thermal Conductivities of Porous Materials," *Journal of Heat Transfer*, Vol. 109, Nov. 1987, pp. 831-834.

¹⁸*Japan Society of Mechanical Engineers Heat Transfer Data Book*, 4th ed., JSME, Tokyo, 1986, p. 184.

¹⁹Takahashi, H., *Elementary Far-Infrared Engineering*, Kogyo-Chosakai, Tokyo, 1988, p. 71.

²⁰Sato, T., *Ferrous Materials*, Asakura-Shoten, Tokyo, 1960, p. 72.

²¹Touloukian, Y. S. (ed.), *Thermophysical Properties of High Temperature Solids*, Vol. 4, Pt. II, Macmillan, New York, 1967, p. 1302.

²²Kamiuto, K., and Iwamoto, M., "Effects of Correlated Scattering on Coupled Heat Transfer by Conduction and Radiation Through a Packed Layer of Glass Beads," *JSME International Journal*, Series II, Vol. 33, No. 12, 1990, pp. 766-771.

Progress in Astronautics and Aeronautics

Gun Muzzle Blast and Flash

Günter Klingenberg and Joseph M. Heimerl

The book presents, for the first time, a comprehensive and up-to-date treatment of gun muzzle blast and flash. It describes the gas dynamics involved, modern propulsion systems, flow development, chemical kinetics and reaction networks of flash suppression additives as well as historical work. In addition, the text presents data to support a revolutionary viewpoint of secondary flash ignition and suppression.

The book is written for practitioners and novices in the flash suppression field: engineers, scientists, researchers, ballisticians, propellant designers, and those involved in signature detection or suppression.

1992, 551 pp, illus, Hardback, ISBN 1-56347-012-8,
AIAA Members \$65.95, Nonmembers \$92.95
Order #V-139 (830)

Place your order today! Call 1-800/682-AIAA



American Institute of Aeronautics and Astronautics

Publications Customer Service, 9 Jay Gould Ct., P.O. Box 753, Waldorf, MD 20604
Phone 301/645-5643, Dept. 415, FAX 301/843-0159

Sales Tax: CA residents, 8.25%; DC, 6%. For shipping and handling add \$4.75 for 1-4 books (call for rates for higher quantities). Orders under \$50.00 must be prepaid. Please allow 4 weeks for delivery. Prices are subject to change without notice. Returns will be accepted within 15 days.